4D RADAR/IMU/GNSS INTEGRATED POSITIONING AND MAPPING FOR LARGE-SCALE ENVIRONMENTS

Binliang Wang[a], Yuan Zhuang[a,*], Nashwa El-Bendary[b]

[a]State Key Laboratory of Information Engineering in Surveying, Mapping, and Remote Sensing, Wuhan University, China
[b]College of Computing and Information Technology,
Arab Academy for Science, Technology, and Maritime Transport (AASTMT), ASWAN-EGYPT

KEY WORDS: 4D imaging radar, Radar Inertial Odometry, Consistent Mapping, GNSS, iEKF.

ABSTRACT:

4D millimeter-wave radar can work in harsh weather conditions such as fog and snow, and measure the position and radial Doppler velocity of objects in three-dimensional space. Some existing methods perform positioning by fusing 3D velocity or point cloud matching information estimated by 4D radar with IMU information. However, the sparsity of radar point clouds and the interference of large amount of noise lead to low accuracy of odometry, and most of the existing work cannot achieve the global consistent mapping with radar point clouds. In this paper, a 4D radar/IMU/GNSS localization and mapping method, G-iRIOM, is proposed. We tightly coupled IMU measurement, Doppler observation information and point cloud matching information from 4D radar by iterative extended Kalman filtering (iEKF) method, and introduced GNSS RTK and loop closure information as global observation to correct the positioning drift of the odometry. The experimental results show that the tightly coupled Doppler velocity information can effectively improve the control of the pose on the local point cloud position, thus enhancing the mapping accuracy. Meanwhile, the introduction of GNSS and loop closure information can significantly improve the positioning accuracy of 4D radar odometry as a kind of global observation, and achieve global consistent mapping of large-scale outdoor scenes based on 4D radar point clouds.

1. INTRODUCTION

Autonomous driving and robotics are popular fields in recent years, and multi-sensor fusion localization and navigation technology is one of the key technologies in them. Lidar and camera are commonly used sensors for autonomous vehicles, but they are difficult to work in bad weather. Millimeter-wave radar has the advantage of resisting interference from rain, snow, etc., and can measure the distance, direction and Doppler velocity of objects in rain, snow and fog. In addition, it can estimate the vehicle's ego-velocity from a single scan.

4D imaging millimeter wave radar improves the resolution in the vertical direction, and thus can better detect obstacle contours, and improve path planning and passable space detection capabilities. Figure 1 shows the mapping result of 4D radar and lidar. However, 4D millimeter wave radar has low spatial resolution compared with cameras or lidars for the moment and the point cloud is relatively sparse. Moreover, it is affected by multipath effects, harmonics and other noise, making it difficult to achieve stable, continuous, and high-precision odometry. Therefore, it is still a challenging task to perform high precision 3D spatial localization and mapping by a 4D millimeter wave radar.

To improve the robustness of odometry and reduce trajectory drift caused by missing data and incorrect matches in scan-to-scan matching, some studies have used inertial data as continuous observations in conjunction with scan-to-scan matching. Many other studies have combined IMU measurements with radar single-scan velocity estimates since 4D radar can estimate 3D ego-velocity from a single scan. In general, scan matching can provide many point constraints, but it is sensitive to measurement noise and matching errors and may fail in areas with sparse radar points. The ego-velocity derived from a radar scan is not affected by drift but is largely unable to correct vertical drift.

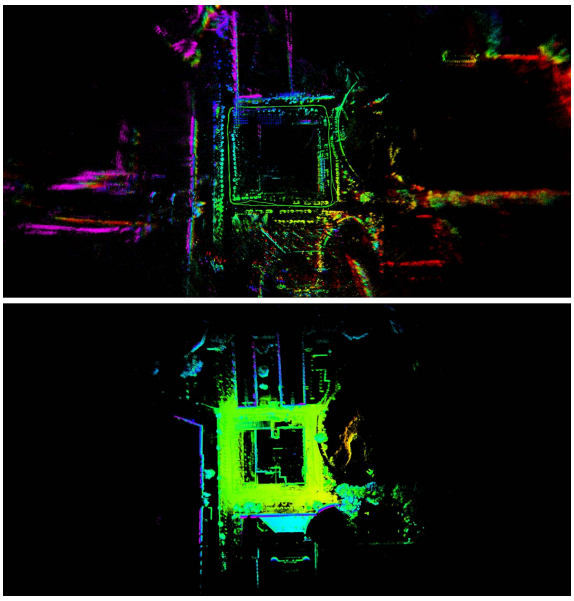

Figure 1. Mapping results of 4D imaging radar and lidar. Map points are colored by the elevation.

Meanwhile, due to the relatively lower angle resolution and accuracy of current 4D radar hardware, the existing 4D radar (inertial) odometey can lead to positioning drift.

To address the issue of positioning drift, we propose an integrated 4D radar/IMU/GNSS positioning and mapping method called G-iRIOM. This method tightly couples IMU information with 4D radar point cloud matching and Doppler observation,

* Corresponding author

and introduces GNSS RTK measurement and loop closure information as the global constraints. The main contributions of this paper are:

1. We tightly coupled IMU information with 4D radar point cloud matching and Doppler information through an iterative Kalman filtering method, while using GNSS information as an observation to further improve the positioning results of radar inertial odometry.

2. We adopt the scan-to-local-map method for point cloud matching to avoid the trajectory drift problem caused by inter-frame matching. We also introduce RCS information to weight the matching for robust and accurate 3D position estimation.

3. We further optimized the local map and pose information obtained from radar odometry through loop closure to ensure the quality of positioning and mapping in the event of GNSS signal occlusion, and achieve large-scale 3D consistent map construction based on 4D imaging radar.

2. RELATED WORK

This section briefly reviews some of the existing methods for radar (inertial) localization and mapping.

3D Radar Odometry. 3D millimeter wave radars can only estimate planar position from distance and azimuth data, lacking object heights due to low elevation resolution. Therefore, most radar odometry methods convert the radar data to a flat image or a 2D point cloud and use image features/direct matching methods to estimate the odometry. The feature-based approach extracts and associates key points by feature descriptors or graph matching. Cen et al. proposed two methods [Cen and Newman, 2018], [Cen and Newman, 2019] to suppress multipath noise and improve robustness of radar scan matching. Barnes et al. [Barnes and Posner, 2020] proposed a self-supervised network to generate key points and descriptors for scan matching, improving the accuracy of radar odometry. Hong et al. [Hong et al., 2020] used classical algorithms (e.g., SURF) to associate scans for pose estimation and loop detection in a radar SLAM system. Burnett et al. [Burnett et al., 2021] used the algorithm in [Cen and Newman, 2019] to build a radar SLAM system and considered motion distortion in the rotating radar data. The direct methods directly register radar scans to estimate the relative pose. Park et al. [Park et al., 2020] applied the Fourier-Melling transform (FMT) to sequential radar scans to estimate rotations and translations. Barnes et al. [Barnes et al., 2020] proposed a correlation-based end-to-end radar odometry, where a mask network removed radar data noise, and the fast Fourier transform (FFT) matching method obtained the relative pose.

4D Radar Inertial Odometry. 4D imaging radars enhance the elevation resolution compared to 3D radars, but their point clouds are still sparse ($\sim$ 400 points/scan). The point cloud matching of 4D imaging radars has a 3D search space instead of 2D, and suffers from various noises, making it hard to achieve stable and accurate scan matching. 4D iRIOM [Zhuang et al., 2023] and 4DRadarSLAM [Zhang et al., 2023] enhanced GICP by considering the probability distribution of the point cloud for more stable scan matching. Some works used inertial data with scan-to-scan matching to make the odometry more robust and reduce trajectory drift for missing data and wrong matches. Almalioglu et al. [Almalioglu et al., 2020] coupled the radar poses from the normal distribution transform and IMU data by an unscented Kalman filter, and used a long short-term memory motion model to estimate 3D ego-motion. Lu et al. [Lu et al., 2020] proposed a deep neural network based radar inertial odometer, which encoded radar data by a convolutional neural network and IMU data by a recurrent neural network, and achieved real-time pose estimation by a multi-modal sensor fusion network. Some other studies fused IMU measurements with radar single-scan velocity estimates from 4D radar. Kramer et al. [Kramer et al., 2020] proposed a robot velocity estimation method based on sliding window optimization to fuse inertial and radar data, estimating the robot's 3D velocity in real time. Doer et al. [Doer and Trommer, 2020a] proposed an EKF-based radar inertial odometry method for 3D localization by fusing IMU and radar ego-velocity estimated by a RANSAC scheme. They also used altimeter data to eliminate altitude drift and introduced online calibration and the Manhattan world assumption as a yaw angle aid [Doer and Trommer, 2021]. Scan matching can provide many point constraints, but is prone to noise and errors, and may fail in sparse radar points. The radar scan-derived ego-velocity is drift-free, but sparsity of constraints and velocity estimation errors tend to lead to vertical drift. In this paper, we directly tightly couple Doppler measurements with scan matching information to enhance the odometry robustness, instead of estimating ego-velocity before fusion.

Loop Closure Detection. Odometry can lead to large localization errors in large-scale environments, so a loop closure detection module is usually needed to correct drift. There are two main types of loop closure detection and relocalization methods for radar-based fusion localization systems: deep learning-based methods, such as [Wang et al., 2021], and traditional geometric methods, such as [Park et al., 2020], [Kim and Kim, 2018]. Deep learning-based methods can achieve good results in specific scenes, but have high computational costs and low generalization abilities. Representative geometry-based methods include scancontext [Kim and Kim, 2018], BoW3D [Cui et al., 2022], etc., which were originally designed for lidar. Scancontext is a method that converts radar scan into a two-dimensional image representation in the BEV view, which can effectively measure the similarity between different scans, and has rotation invariance and scale invariance.

3. METHODOLOGY

The architecture of the proposed 4D radar/IMU/GNSS integrated system is shown in Figure 2. The system inputs are time-aligned radar, IMU, and GNSS RTK data. Due to the small number of points in a single radar scan and the presence of moving interference points and noise points caused by multipath and scattering, we first remove noise points from the radar to achieve data enhancement. Secondly, we use IMU to predict the propagation vehicle state (position, attitude, velocity, etc.) and iteratively update the state using an extended Kalman filter algorithm tightly coupled with radar point cloud matching and Doppler measurement. Then, we update the vehicle state with GNSS RTK information to further eliminate odometry positioning drift. Finally, we perform loop closure detection using improved scancontext, called submapcontext, to obtain loop constraints and perform pose graph optimization to obtain a refined vehicle state and a globally consistent map.

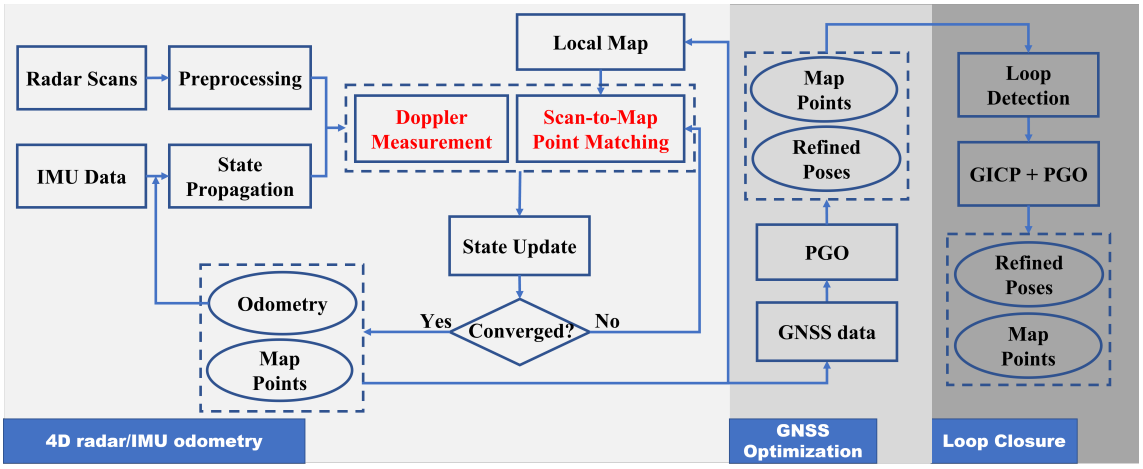

Figure 2. System overview of G-iRIOM.

3.1 State Definition

In the state estimated process, $\mathbf{x}$ is the state, $\mathbf{u}$ is the control input (i.e., IMU observations), and $\mathbf{w}$ is the system noise.

$$\begin{aligned}\mathbf{x} &= \left[{}^{G}\mathbf{p}_I^T, {}^{G}\mathbf{v}_I^T, {}^{G}\mathbf{R}_I^T, \mathbf{b}_a^T, \mathbf{b}_\omega^T, {}^{I}\mathbf{R}_R^T, {}^{I}\mathbf{l}_R^T, {}^{G}\mathbf{g}^T\right]^T \\ \mathbf{u} &= \left[\mathbf{a}_m^T, \boldsymbol{\omega}_m^T\right] \\ \mathbf{w} &= \left[\mathbf{n}_a^T, \mathbf{n}_\omega^T, \mathbf{n}_{ba}^T, \mathbf{n}_{b\omega}^T\right]\end{aligned} \tag{1}$$

where ${}^{G}\mathbf{p}_I, {}^{G}\mathbf{v}_I, {}^{G}\mathbf{R}_I$ is the position, velocity, and attitude of the IMU in the world coordinate system. $\mathbf{b}_a, \mathbf{b}_\omega$ is the IMU bias, modeled as a random walk process with Gaussian noise $\mathbf{n}_a, \mathbf{n}_\omega$. ${}^{I}\mathbf{R}_R, {}^{I}\mathbf{l}_R$ are the external orientation elements between the radar and IMU coordinate system. ${}^{G}\mathbf{g}$ is the gravity vector in the world coordinate system. $\mathbf{a}_m, \boldsymbol{\omega}_m$ are the linear acceleration and angular velocity observations of IMU with observation noise of $\mathbf{n}_a, \mathbf{n}_\omega$.

3.2 Doppler Velocity Measurement

Frequency modulated continuous wave (FMCW) radar can usually provide Doppler velocity observations, which measure the magnitude of the projection of the relative velocity between a detected target and the radar in the target's radial direction. Similarly, we can project the ego-velocity obtained by the algorithm to that direction by the target point's position in the radar body frame. Ideally, they are equal. Thus, we can construct the Doppler observation residual equation as follows:

$$r_v^d = v^d - v_m^d \approx \widehat{r}_v^d + \mathbf{H}_v\widetilde{\mathbf{x}} \tag{2}$$

$$v^d = \boldsymbol{\rho}^T/||\boldsymbol{\rho}|| \cdot {}^{R}\mathbf{v} \tag{3}$$

$${}^{R}\mathbf{v} = {}^{I}\mathbf{R}_R^T\left({}^{G}\mathbf{R}_I^T{}^{G}\mathbf{v}_I + (\boldsymbol{\omega}_m - \mathbf{b}_\omega)_\times {}^{I}\mathbf{l}_R\right) \tag{4}$$

where r_v^d is the residual and $\mathbf{H}_v$ is the Jacobian matrix of r_v^d relative to the error state $\widetilde{\mathbf{x}}$. v^d and v_m^d is the Doppler velocity and its observation, $\boldsymbol{\rho}$ is the position of the target observation in the radar body frame, and $||\boldsymbol{\rho}||$ is its norm. ${}^{R}\mathbf{v}_m$ is the radar ego-velocity in the radar body frame.

Compared with the loosely coupled approach used by the 4D iRIOM [Zhuang et al., 2023] and EKFRIO [Doer and Trommer, 2020b] methods, we establish the 1D residual equations for the radar observations directly from the original Doppler velocity measurements, without using methods such as least squares to calculate the radar ego-velocity observations (3D) for a single frame in advance. This tightly coupled approach makes the Doppler velocity constraint more uniform and dense, effectively enhancing the consistency between the optimized state and the local observations.

3.3 Radar Point Matching

As in 4D iRIOM [Zhuang et al., 2023], we use a scan-to-submap matching method and a distribution-to-multi-distribution spatial weighting strategy. On this basis, we use RCS to weight the radar point matching residuals defined in iRIOM, thus reducing the impact of matches with large RCS differences on the state updating process, as we consider these matches to be unreliable. The RCS-weighted matching residual is given by:

$$\mathbf{r}_p = \mathbf{W}_{rcs} \cdot \mathbf{G}_p(\Sigma_j({}^{G}\mathbf{b}_j/N) - {}^{G}\mathbf{T}_R \cdot {}^{R}\mathbf{a}) \tag{5}$$

$$\mathbf{W}_{rcs} = exp(-\lambda \cdot \sum\nolimits_j ||RCS(\mathbf{b}_j) - RCS(\mathbf{a})||) \tag{6}$$

where ${}^{R}\mathbf{a}$ is a point in the current scan, ${}^{G}\mathbf{b}_j$ $(j = 1, \ldots, N)$ are the N nearest neighbor points, $RCS(\mathbf{a})$ and $RCS(\mathbf{b}_j)$ are their RCS measurements. ${}^{G}\mathbf{T}_R$ is the transformation matrix from radar coordinate system to global coordinate system.

Similarly, we perform a linear expansion of $\mathbf{r}_p$ as follows:

$$\mathbf{r}_p \approx \widehat{\mathbf{r}}_p + \mathbf{H}_p\widetilde{\mathbf{x}} \tag{7}$$

$$\mathbf{H}_p = \begin{bmatrix}\mathbf{G}_p & \mathbf{0}_3 & \mathbf{H}_p^R & \mathbf{0}_3 & \mathbf{0}_3 & \mathbf{H}_p^{R_e} & \mathbf{H}_p^l & \mathbf{0}_3\end{bmatrix} \tag{8}$$

$$\mathbf{H}_p^R = \mathbf{W}_{rcs}\mathbf{G}_p\left({}^{G}\mathbf{R}_I\left({}^{I}\mathbf{R}_R \cdot {}^{R}\mathbf{a} + {}^{I}\mathbf{l}_R\right)\right)_\times \tag{9}$$

$$\mathbf{H}_p^{R_e} = \mathbf{W}_{rcs}\mathbf{G}_p{}^{G}\mathbf{R}_I\left({}^{I}\mathbf{R}_R \cdot {}^{R}\mathbf{a}\right)_\times \tag{10}$$

$$\mathbf{H}_p^l = -\mathbf{W}_{rcs}\mathbf{G}_p{}^{G}\mathbf{R}_I \tag{11}$$

where $\widehat{\mathbf{r}}_p$ and $\mathbf{H}_p$ are the computed residual and the Jacobian matrix relative to the state. $(\cdot)_\times$ is skew-symmetric matrix.

3.4 State Optimization

As mentioned before, the state optimization process mainly consists of three parts: radar inertial odometry, GNSS pose graph optimization, and loop closure optimization.

Radar inertial odometry. We first predict and propagate the robot state by integrating the IMU data, then obtain the Doppler velocity observation and the scan-to-submap point cloud matching pairs based on the predicted state and the preprocessed radar data, and construct the corresponding residual constraints (as in III-B and III-C). Then we use the iEKF method to iteratively update the state and obtain the odometry pose results.

GNSS pose graph optimization. The pose obtained from the odometry are the input of GNSS pose map optimization module, We construct the relative pose factor from the odometry results and the absolute position factor from the GNSS measurement. Based on Ceres Solver, we construct and solve the pose factor optimization problem.

Loop closure optimization. The poses and point clouds obtained by GNSS optimization are further fed to the loop closure detection module. We use an enhanced version of the scancontext algorithm, named submapcontext, for loop closure detection. The point cloud from a single radar scan is sparse and has low quality for direct feature extraction and matching. Therefore, we fuse the point clouds from several neighboring scans of the current scan to form a submap, and perform feature extraction, retrieval and matching. Then, similar to the GNSS optimization module, we construct odometry relative pose factors and loop closure relative pose factors, and use Ceres Solver to solve for the current pose graph.

4. EXPERIMENTS

4.1 Experimental Setup and Data

We installed a 4D radar ARS548 from Continental on a ground robot, which operates in the $76-77$ GHz band and scans at 15 Hz. It has a vertical AOV of $\pm 20^{\circ}$ and a horizontal AOV of $\pm 60^{\circ}$, with an angular resolution of 0.2° in azimuth and 0.1° in elevation. It can detect objects up to about $\sim$300 m away with an accuracy of 0.3 m. We obtained the reference trajectory from the Bynav X1-5H GNSS/INS module in areas with clear sky. We fused the IMU and GNSS data from the built-in IMU (EPSON G345) and GNSS RTK of the Bynav module with the radar data.

To evaluate the performance of our algorithm, we conducted data collection and verification in an outdoor open scene and a scene with partial GNSS occlusion. Dataset 1 is an outdoor basketball court with a duration of 6 minutes. GNSS RTK measurements were available throughout. Dataset 2 was collected by traversing around the Xinghu Building of LIESMARS for two laps. The occlusion of high-rise buildings prevents the GNSS signal in some areas.

4.2 Results Evaluation

All two experimental datasets start and stop at the same pose, so we can evaluate the algorithm performance by the trajectory closure error (CE). To verify the repeatability of the algorithm, we ran 10 times on each dataset and calculated the mean value of the closure error. Meanwhile, we evaluate the accuracy of the method by calculating the difference between the algorithm's results and the reference trajectory. We take the centimeter-level trajectory obtained by the fusion of GNSS and IMU as the reference trajectory, and evaluate the pose esmation accuracy of the algorithm by calculating the root mean square error (RMSE) between the reference trajectory and the algorithm results, including absolute pose error (APE) and relative pose error (RPE).

We compare our G-iRIOM method with the EKFRIO method [Doer and Trommer, 2020b], which is the best-known and open-source 4D radar inertial odometry method. Moreover, we compare two variants of our previously proposed 4D radar inertial mapping and positioning method [Zhuang et al., 2023]: the iRIO method without the loop closure module and the iRIOM method with the loop closure module. Furthermore, to test the competitiveness of our radar-based multi-sensor fusion localization method with the existing popular lidar method, we compare it with the FastLIO-SLAM method that fuses loop closure information.

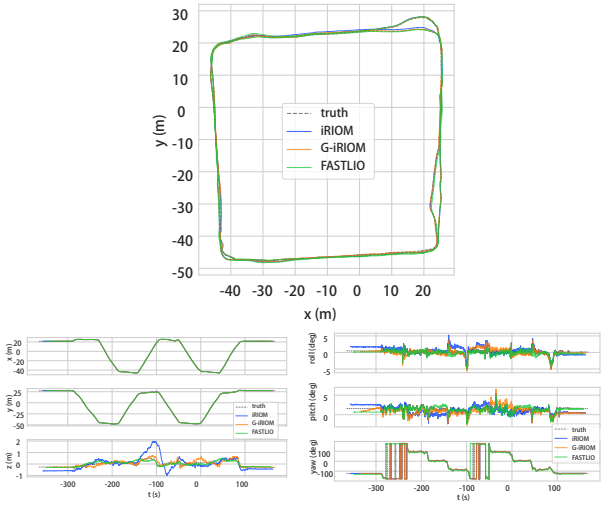

Figure 3. Top: Trajectories estimated by the iRIOM, G-iRIOM, FastLIO-SLAM on our dataset 2. Bottom: The position and attitude of estimated trajectories by these methods aligned to the reference.

The accuracy statistics corresponding to the experimental results are shown in Table I. We can see that the iRIOM method with loop closure significantly improves the localization accuracy over the EKFRIO and iRIO methods, while the G-iRIOM method with fused GNSS measurements further reduces the closure error and absolute position error in all scenes, effectively enhancing the positional recovery accuracy. Compared with the FastLIO-SLAM method based on Velodyne VLP-16 lidar data, the G-iRIOM localization performance is comparable on these data sequences.

Figure 3 illustrates the trajectory estimation results of these methods for dataset 2 and their comparison with the ground truth. In Figure 4, the visualization results demonstrate that the G-iRIOM method can enhance the consistency of 4D radar mapping and reduce the closure error.

4.3 Ablation Studies

To verify the effects of IMU data, radar doppler velocity measurements, radar point cloud matching, loop closure information, and GNSS measurements, we tested the proposed method on the aforementioned data sequences by turning off one type of measurement or constraint.

Table II shows the trajectory closure error as well as the trajectory RMSEs for the ablation experiments. Figure 4 shows

	Method	Closure Error		APE RMSE		RPE RMSE	
		Horizontal (m)	Vertical (m)	Translation (m)	Rotation (°)	Translation (%)	Rotation (°/m)
Dataset 1	EKFRIO	0.530	15.759	5.616	10.261	0.055	0.183
	iRIO	0.029	0.010	0.313	2.923	0.040	0.171
	iRIOM	0.027	0.010	0.305	2.751	0.040	0.171
	G-iRIOM	0.020	0.011	0.198	2.880	0.027	0.199
	FastLIO	0.024	0.007	0.147	5.331	0.025	0.343
Dataset 2	EKFRIO	17.194	24.631	10.068	9.859	0.026	0.120
	iRIO	1.517	5.073	1.518	2.866	0.022	0.114
	iRIOM	0.251	0.113	0.346	2.597	0.022	0.113
	G-iRIOM	0.164	0.016	0.279	2.865	0.018	0.112
	FastLIO	0.151	0.025	0.372	6.363	0.020	0.322

[a] FastLIO denotes FastLIO-SLAM with loop closure.

Table 1. Statistics of EKFRIO, iRIO, iRIOM , G-iRIOM and FastLIO-SLAM on dataset 1-2

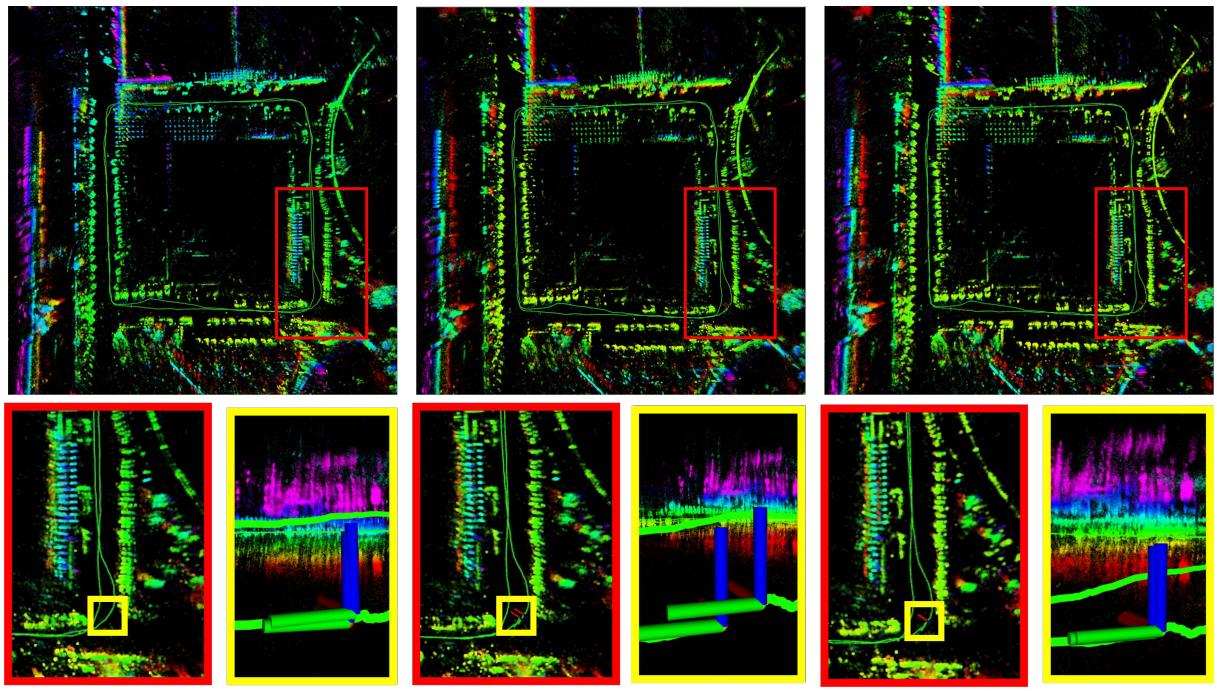

Figure 4. G-iRIOM mapping results on dataset 2 (right), as well as mapping results with no GNSS (left) and no loop closure (middle) information, where points are colored by height.

	TOM	F	Closure Error		RMSE APE		RMSE RPE	
			Horizontal (m)	Vertical (m)	Translation (m)	Rotation (°)	Translation (%)	Rotation (°/m)
1	IMU	5	23.532	2.165	9.112	8.302	0.100	0.298
	DVM	1	0.356	0.003	0.271	3.425	0.028	0.200
	S2M	1	1.670	0.188	2.551	25.325	0.027	0.132
	LCI	0	0.026	0.113	0.169	3.010	0.026	0.201
	GNSS	0	0.045	0.029	0.174	2.994	0.026	0.201
2	IMU	2	6.012	8.367	4.791	3.528	0.039	0.236
	DVM	1	0.504	0.079	0.667	3.638	0.020	0.212
	S2M	0	0.704	0.807	1.799	7.060	0.032	0.180
	LCI	0	0.850	0.394	0.629	3.430	0.018	0.213
	GNSS	0	0.204	0.164	0.490	3.466	0.020	0.212

[a] IMU: imu data measurement, DVM: doppler velocity measurement, S2M: scan-to-submap matching constraint, LCI: loop closure information, GNSS: GNSS RTK information.

[b] TOM means the type of measurement turned off, F means the number of failures in 10 repetitions.

Table 2. Ablation Test Statistics on Dataset 1-2

the trajectory estimation performance of the G-iRIOM method when GNSS or loop closure information is not considered. From Table II, we can see that:

(1) When IMU data are unavailable and state prediction is performed by the constant velocity model, the system's positioning accuracy and stability is significantly reduced. The constant velocity model can achieve good state prediction under normal motion, but it often fails to accurately predict the angular velocity at corners, which results in the odometey-predicted pose deviating from the true trajectory.

(2) Odometry stability was reduced when Doppler velocity measurements were not used. The statistical frequency of odometry failure in the middle of all data sequences exceeded 10% in 10 replicate runs.

(3) Odometry closure errors of the these sequences are large when radar point cloud matching was not used and the APE RMSE in position exceeds 1.5 m.

(4) When GNSS or loop closure information are not used, the trajectory closure error of the algorithm becomes significantly larger. As shown in Figure 4, GNSS measurements make the global elevation information more consistent and reduce the offset and drift in the Z-direction (colors related to height are more consistent in the horizontal plane), but cannot guarantee trajectory closure. The opposite is true for the loop closure information. Therefore, effectively combining the two can improve the positioning accuracy.

5. CONCLUSIONS

We propose a 3D spatial motion estimation and mapping method using 4D radar as the primary sensor. The method integrates IMU observation, radar doppler velocity measurement, scan-to-submap matching, loop closure detection information and GNSS position measurement. The 4D radar and IMU data provide accurate local positioning and map point information, while the loop closure detection and GNSS information provide global position observation information, which can effectively reduce the positioning drift of radar inertial odometry. Experimental results demonstrate that the method achieves high accuracy motion estimation. The algorithm is robust to data noise and moving objects, and performs well in localization and mapping experiments for large-scale harsh environments.

REFERENCES

Almalioglu, Y., Turan, M., Lu, C. X., Trigoni, N., Markham, A., 2020. Milli-RIO: Ego-motion estimation with low-cost millimetre-wave radar. *IEEE Sensors Journal*, 21(3), 3314–3323.

Barnes, D., Posner, I., 2020. Under the radar: Learning to predict robust keypoints for odometry estimation and metric localisation in radar. *2020 IEEE Int. Conf. on Robotics and Automation (ICRA)*, IEEE, Virtual, 9484–9490.

Barnes, D., Weston, R., Posner, I., 2020. Masking by moving: Learning distraction-free radar odometry from pose information. *Proc. Conf. Robot Learn.*, PMLR, 303–316.

Burnett, K., Schoellig, A. P., Barfoot, T. D., 2021. Do we need to compensate for motion distortion and Doppler effects in spinning radar navigation? *IEEE Robotics and Automation Letters*, 6(2), 771–778.

Cen, S. H., Newman, P., 2018. Precise ego-motion estimation with millimeter-wave radar under diverse and challenging conditions. *2018 IEEE Int. Conf. on Robotics and Automation (ICRA)*, IEEE, Brisbane, Australia, 6045–6052.

Cen, S. H., Newman, P., 2019. Radar-only ego-motion estimation in difficult settings via graph matching. *2019 Int. Conf. on Robotics and Automation (ICRA)*, IEEE, Montreal, QC, Canada, 298–304.

Cui, Y., Chen, X., Zhang, Y., Dong, J., Wu, Q., Zhu, F., 2022. Bow3d: Bag of words for real-time loop closing in 3d lidar slam. *IEEE Robotics and Automation Letters*, 8(5), 2828–2835.

Doer, C., Trommer, G. F., 2020a. An EKF based approach to radar inertial odometry. *2020 IEEE Int. Conf. on Multisensor Fusion and Integration for Intelligent Systems (MFI)*, IEEE, Karlsruhe, Germany, 152–159.

Doer, C., Trommer, G. F., 2020b. Radar inertial odometry with online calibration. *2020 European Navigation Conference (ENC)*, IEEE, Dresden, Germany, 1–10.

Doer, C., Trommer, G. F., 2021. Yaw aided radar inertial odometry using manhattan world assumptions. *2021 28th Saint Petersburg Int. Conf. on Integrated Navigation Systems (ICINS)*, IEEE, St. Petersburg, Russia, 1–9.

Hong, Z., Petillot, Y., Wang, S., 2020. Radarslam: Radar based large-scale SLAM in all weathers. *2020 IEEE/RSJ Int. Conf. on Intelligent Robots and Systems (IROS)*, IEEE, Las Vegas, USA, 5164–5170.

Kim, G., Kim, A., 2018. Scan context: Egocentric spatial descriptor for place recognition within 3D point cloud map. *2018 IEEE/RSJ Int. Conf. on Intelligent Robots and Systems (IROS)*, IEEE, Madrid, Spain, 4802–4809.

Kramer, A., Stahoviak, C., Santamaria-Navarro, A., Agha-Mohammadi, A.-A., Heckman, C., 2020. Radar-inertial ego-velocity estimation for visually degraded environments. *2020 IEEE Int. Conf. on Robotics and Automation (ICRA)*, IEEE, Virtual, 5739–5746.

Lu, C. X., Saputra, M. R. U., Zhao, P., Almalioglu, Y., De Gusmao, P. P., Chen, C., Sun, K., Trigoni, N., Markham, A., 2020. Milliego: Single-chip mmwave radar aided egomotion estimation via deep sensor fusion. *Proceedings of the 18th Conference on Embedded Networked Sensor Systems*, 109–122.

Park, Y. S., Shin, Y.-S., Kim, A., 2020. Pharao: Direct radar odometry using phase correlation. *2020 IEEE Int. Conf. on Robotics and Automation (ICRA)*, IEEE, Virtual, 2617–2623.

Wang, W., de Gusmao, P. P., Yang, B., Markham, A., Trigoni, N., 2021. Radarloc: Learning to relocalize in FMCW radar. *2021 IEEE Int. Conf. on Robotics and Automation (ICRA)*, IEEE, Xi'an, China, 5809–5815.

Zhang, J., Zhuge, H., Wu, Z., Peng, G., Wen, M., Liu, Y., Wang, D., 2023. 4dradarslam: A 4d imaging radar slam system for large-scale environments based on pose graph optimization. *2023 IEEE International Conference on Robotics and Automation (ICRA)*, IEEE, 8333–8340.

Zhuang, Y., Wang, B., Huai, J., Li, M., 2023. 4D iRIOM: 4D Imaging Radar Inertial Odometry and Mapping. *IEEE Robotics and Automation Letters*.